ISMAR03 in Tokyo, Japan, pp.103-112 (2003)

Personal Positioning based on Walking Locomotion Analysis with Self-Contained Sensors and a Wearable Camera

Masakatsu Kourogi† Takeshi Kurata†‡

†National Institute of Advanced Industrial Science and Technology(AIST)
1–1–1 Umezono, Tsukuba Chuo Dai 2, Tsukuba, Ibaraki, 305–8568, JAPAN

‡University of Washington

E-mail: m.kourogi@aist.go.jp, kurata@ieee.org

Abstract

In this paper, we propose a method of personal positioning for a wearable Augmented Reality (AR) system that allows a user to freely move around indoors and outdoors. The user is equipped with self-contained sensors, a wearable camera, an inertial head tracker and display. The method is based on sensor fusion of estimates for relative displacement caused by human walking locomotion and estimates for absolute position and orientation within a Kalman filtering framework. The former is based on intensive analysis of human walking behavior using self-contained sensors. The latter is based on image matching of video frames from a wearable camera with an image database that was prepared beforehand.

keywords : personal positioning, pedometer, human walking analysis, sensor fusion

1 Introduction

In recent years, wearable computing [2] has become more feasible due to the rapid progress that has been made in lowering the battery consumption and reducing the size and weight to produce compact, lightweight computers and I/O peripherals such as displays, cameras and sensors. Through these wearable computing technologies, it is possible to construct a wearable Augmented Reality (AR) system that allows the user to move freely around a large scale environment.

In this paper, we have aimed at developing this wearable AR (Augmented Reality) system that also receives location/orientation awareness services.

Feiner et al. used a combination of a DGPS (Differential Global Positioning System), magnetometers and inertial head tracker to achieve a mobile AR system that provided a navigation and annotation overlay for outside environments [3]. However, in an indoor environment such as offices and exhibition halls, the GPS signals are easily blocked by the building structure, and the earth's magnetic field is disturbed by electronic devices and appliances such as copiers and CRTs, which makes magnetometers unreliable. Moreover, in an indoor environment, highly accurate estimates of location are required, which are difficult to achieve with GPS/DGPS-based systems.

Newman et al. deployed a set of ultrasonic receivers covering the entire indoor environment and attached an ultrasonic transmitter, an inertial head tracker and a wireless network device to the user to acquire his location and orientation within a covered environment [4]. However, it is still difficult to deploy receivers entirely in a large-scale environment as an infrastructure because of initial deployment and maintenance costs.

Aoki et al. proposed a method of personal positioning based on dynamic programming matching between a time sequence of color histograms of successive images and a database of sequences captured and registered beforehand [5]. In general, methods of personal positioning exploiting images have an advantage in that no surrounding infrastructure is required. However, image-based methods require a database for registration covering the entire location where the user can go within it. Needless to say, this is very time-consuming to construct and difficult to apply to a large scale environment.

However, the Inertial Navigation System (INS), which is a source-independent location/orientation estimation system, has been used by aircraft and submarines for navigation purposes. Through the introduction of Micro-Electro Mechanical System (MEMS) technologies, the inertial sensors incorporated in the INS have dramatically been downsized and packaged into a single unit called the Inertial Measurement Unit (IMU). These units are readily available from several vendors such as Crossbow Technology [7] and American GNC [8]. However, for personal and wearable uses, they are still too large, heavy and expensive to achieve the required accuracy for personal navigation indoors. INS also requires a lengthy initialization sequence called ZUPT (Zero Velocity Update) hindering immediate use.

Many researchers have proposed multi-sensor based methods aimed at human-specific behaviors for personal positioning. Golding et al. proposed an indoor navigation method based on a statistical analysis of multi-sensor data such as accelerometers, magnetometers, thermometers and light sensors [6]. However, since it takes some time to acquire statistically meaningful results from multi-sensor data, it cannot easily be used for real-time applications.

Judd et al. developed a light-weight and mobile dead-reckoning module that detects human walking steps and estimates the step length based on the peak detection of vertical acceleration changes and its frequency analysis. It also senses the direction with magnetometers [9][10]. The module is already available from Point Research Corporation [11]. However, the earth's magnetic field can be unreliable in an indoor

environment. Moreover, it assumes that human walking is continuous for a certain period of time.

Lee et al. proposed an incremental positioning method based on detecting of human walking behavior through accelerometers and the walking direction through magnetometers [12]. Although it estimates the relative displacement of the user, it can only be used for a limited range for which the paths of displacement have been pre-registered. It also requires absolute positioning information from an external source and a mechanism of data integration between relative displacement and absolute positioning, which cannot be done with this method.

We took the approach of combining the measurement of relative displacement by analyzing human locomotion on foot and several other methods of absolute positioning within a Kalman filtering framework. First, we attached self-contained sensors to the user's torso (the pelvis) to detect and measure his displacement achieved by analyzing a pattern of the acceleration vector and angular velocity vector caused by walking behavior. The sensors were composed of 3-axis accelerometers, gyro-sensors and magnetometers. Thanks to advanced MEMS technologies, these sensors were very tiny and inexpensive and were able to be packaged into a single package that was as small as a typical cellular phone.

Clinical studies of human movement have revealed that the pattern of movement and applied force to the center of gravity (COG) of the human body (COG is located near the pelvis) while walking is almost deterministic and undisturbed by individual characteristics [13]. We can thus detect and measure human walking behavior by analyzing a time sequence of the acceleration vector and angular velocity vector without introducing a learning mechanism to absorb individual differences. Second, we can use a wearable camera and an inertial head tracker to determine absolute positioning and head orientation. The wearable camera is attached to the user's head and aligned to match his direct of sight. A set of images taken at several points in the environment are stored beforehand as a database that is associated with the position and orientation of capture. We matched the image from the wearable camera with that in the database through frame-to-frame image registration [14]. If image matching was successful, we acquired the direction of the user's head and his absolute position.

This paper first describes a method of detecting and measuring a unit cycle of walking locomotion and walking direction achieved by analyzing the acceleration vector, angular velocity vector and magnetic vector acquired from self-contained sensors. We exploited our knowledge of the dip angle, which was uniquely determined by the latitude and longitude of the location to handle disturbances of the magnetic field [15].

It then describes a method of integrating the measurement of relative displacement and absolute positioning within a Kalman filter framework.

Finally, it discusses implementation of the proposed method through a wearable prototype system called *Wyvern* [1], and ends with an evaluation of the accuracy of the positioning system.

2 Dead-reckoning based on human locomotion

In this section, we first discuss how displacement caused by human walking locomotion can be estimated. We handle three types of locomotion. There are:

1. Walking on a flat floor,
2. Going up or down stairs, and
3. Taking an elevator.

Most perambulation through exhibition halls and offices is covered by these types.

Figure 1 has a typical pattern for vertical and forward acceleration caused by human walking locomotion on a flat floor. The definition of each axis is in Figure 2. We notice that there is a very simple pattern similar to sine waves with different phases but at the same frequency (Figure 1).

Note that these time signal data were acquired from a single package of self-contained sensors. It was the 3DM-G from MicroStrain Inc. [17], and was used throughout the study. Acceleration was processed with a low-pass filter (FIR1-type, 10-steps, cut-off frequency: 1/5), and angular velocity with a low-pass filter (FIR1-type, 10-steps, cut-off frequency: 2/5) to

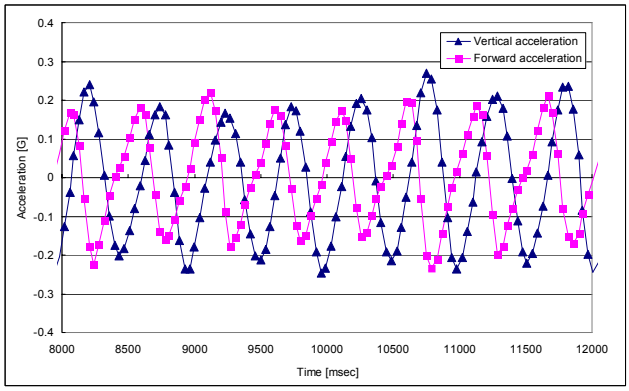

Figure 1: Typical pattern of vertical and forward acceleration walking locomotion on flat floor.

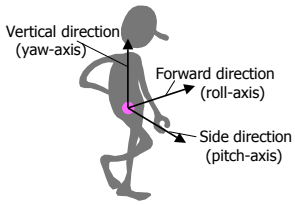

Figure 2: Definition of each axis.

Figure 3 has the definition of a unit cycle of walking behavior, and the relationship between the stage of the walking cycle and the change in vertical and forward acceleration.

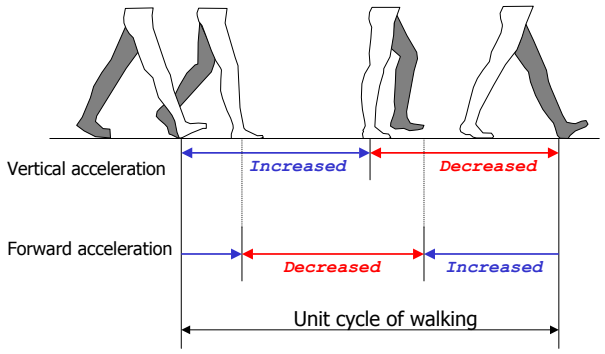

Figure 3: Walking stage and acceleration pattern.

Figure 4 has a detailed analysis of the pattern in Figure 3, especially the time positions for the positive and negative peak of each signal. It is obvious that the negative peak for vertical acceleration is quickly followed by the positive peak for forward acceleration. It can also be noticed that the gradient of forward acceleration from the positive to the negative peak is sharper than that from the negative to the positive peak. This phenomenon is not observed in the gradient difference in vertical acceleration.

Therefore, peak detection and a gradient test algorithm for both vertical acceleration and forward acceleration are essential to detect a unit cycle of walking

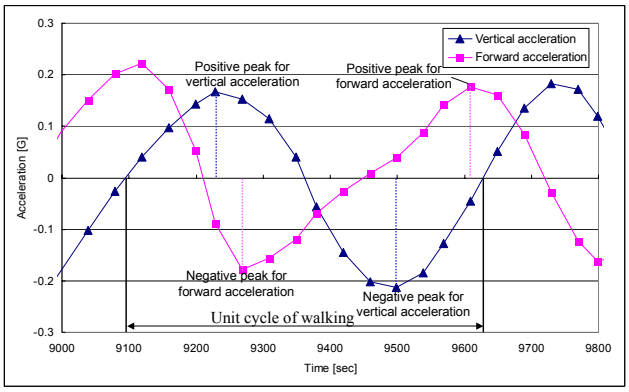

Figure 4: Analysis of unit cycle of acceleration.

2.1 Estimate of gravitational vector

It is necessary to estimate the direction of gravity not only to remove the gravitational acceleration vector from the total acceleration vector but also to adjust the effect of attitude changes on the attached sensors while walking. To estimate the gravitational vector, we used the acceleration vector and angular velocity vector as a source of information. We used a Kalman filter framework [18][19] to fuse this information, and regarded the acceleration vector and angular velocity vector as measurement vector, and regarded the gravitational acceleration vector and angular velocity vector as state vector.

Therefore, the prediction equations of the state vector from discrete time t to $t+1$ are as follows:

$$g_{x|t+1} = g_{x|t} - (\omega_{y|t} g_{z|t} - \omega_{z|t} g_{y|t})\Delta t, \quad (1)$$

$$g_{y|t+1} = g_{y|t} - (\omega_{z|t} g_{x|t} - \omega_{x|t} g_{z|t})\Delta t, \quad (2)$$

$$g_{z|t+1} = g_{z|t} - (\omega_{x|t} g_{y|t} - \omega_{y|t} g_{x|t})\Delta t, \quad (3)$$

where $(g_{x|t}, g_{y|t}, g_{z|t})$ is the gravitational vector and $(\omega_{x|t}, \omega_{y|t}, \omega_{z|t})$ is the angular velocity vector at t.

We collected a data set of the acceleration vector to acquire the covariance matrix of the measurement noise vector of gravitational acceleration by walking on flat floor, standing still, and going up/down stairs and calculating the covariance matrix.

By using the gathered data in such ways, the Kalman filter is thought to work especially well in walking behaviors. And as for covariance matrix about the angular velocity, we use the specification datasheet of the gyro-sensors.

We constructed a software inclinometer from the gyro-sensors and accelerometers using the method described in this section.

2.2 Detection of the forward direction

We need to establish the forward direction relative to the sensors, since this is not known initially. Thus, it is necessary to calibrate the sensor after it is attached to the user.

Figure 5 shows the distribution of a time series for the planar acceleration vector (a_x, a_y) where a_x is the side acceleration and a_y is the forward acceleration.

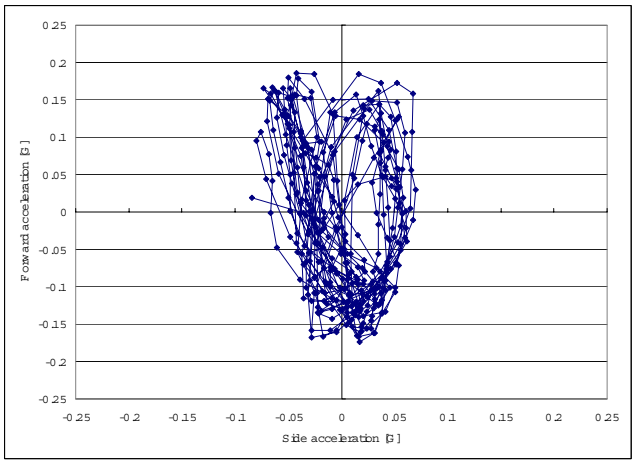

Figure 5: Typical distribution pattern for side and forward acceleration.

In this figure, we notice that the principal component vector of the planar acceleration vector is along

the forward-and-backward direction. To estimate the direction, we first removed the gravitational acceleration vector estimated with this method (described in Section 2.1) from the total acceleration vector. Second, we computed the projected vector component along with the gravitational direction and removed it from the gravitation-free acceleration vector obtained above. We then acquired the residual acceleration vector at each sampling time which should be the horizontal acceleration vector. By applying Principal Component Analysis (PCA) to the time series for the residual acceleration vector, the axis for the forward-and-backward direction can be estimated from the statistically determined principal component vector (d_x, d_y, d_z). The secondary principal component should be the right-angle side direction. To determine which is the forward direction, we used our knowledge of the pattern for forward and vertical acceleration shown in Figure 4. The positive peak for forward acceleration is located at the middle of the sharply increasing slope for vertical acceleration at the same time. We can determine the forward direction by testing whether the slope of vertical acceleration at the peak for forward acceleration is increasing. Figure 6 is a schematic diagram used to estimate the forward-and-backward direction.

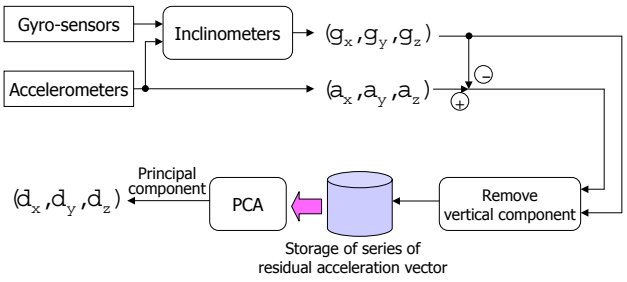

Figure 6: Diagram to estimate forward-and-backward direction.

2.3 Detection of unit cycle of walking behavior

Using the estimated vertical (gravitational) and forward directions of the sensors using the previously described methods, the measured acceleration vector can be decomposed into each component. As Figure 4 shows, in a unit cycle of walking behavior, the positive peak for vertical acceleration should be followed by the negative peak, and the negative peak for forward acceleration is followed by the positive peak. We first detected a pair of positive-negative peaks for vertical acceleration and stored a time series for forward acceleration. Once detected, we searched for a pair of negative-positive peaks for forward acceleration from storage. If found, we tested the gradient for forward acceleration from the positive to the negative peak based on our knowledge that the gradient should be sharp. We thus tested if the gradient was above a threshold, and determined if a unit cycle of walking

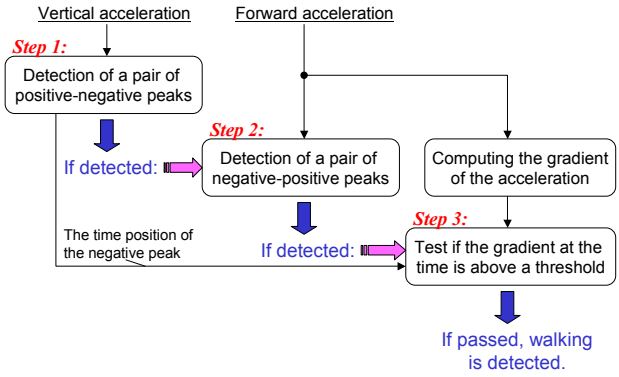

Figure 7: Diagram of detecting unit cycle of walking.

2.4 Measuring walking velocity and step length

It is known empirically that the differences between the positive and negative peak for vertical acceleration and forward direction have strong a correlation with walking velocity.

Figure 8 shows the relationship between the forward acceleration differences and the walking speed tested by subjects A and B. By regression analysis with these data, we obtained each correlation coefficient $R_{f,A} = 0.988$ and $R_{f,B} = 0.986$ for subjects A and B, respectively. We also obtained slopes and intercepts for subjects A and B. These were $a_{f,A} = 6.52$, $a_{f,B} = 7.35$, $b_{f,A} = 1.78$ and $b_{f,B} = 1.24$, where $Y = aX_f + b$, and Y was the walking speed and X_f was the forward acceleration difference between top

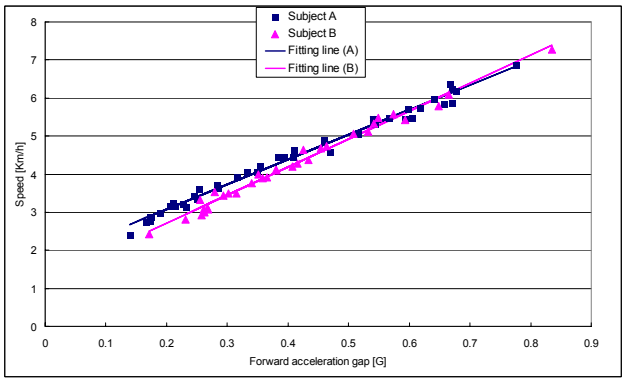

Figure 8: Relationship between forward acceleration difference and walking speed (by subjects A and B).

Figure 9 shows the relationship between the vertical acceleration differences and the walking speed tested by subjects A and B. Through regression analysis with these data, we obtained each correlation coefficient

$R_{v,A} = 0.940$ and $R_{v,B} = 0.880$ for subjects A and B, respectively. We also obtained slopes and intercepts for subjects A and B, which were $a_{v,A} = 20.25$, $a_{v,B} = 31.09$, $b_{v,A} = -1.13$ and $b_{v,B} = -2.62$, where $Y = aX_v + b$, and Y is the walking speed and X_v is the vertical acceleration difference between the top and bottom peak. These results indicate that individual differences play slight roles when estimating the walking speed from acceleration.

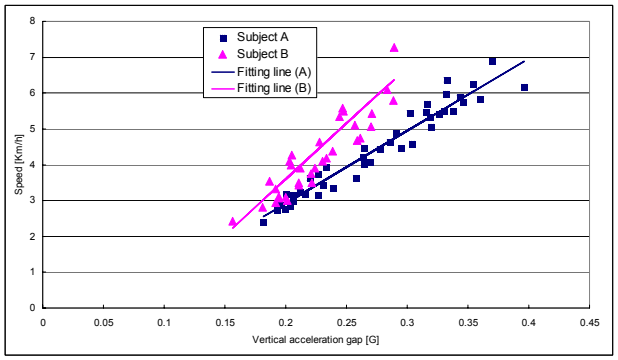

Figure 9: Relationship between vertical acceleration difference and walking speed (by subjects A and B).

The step length can be computed by multiplying the walking speed by the time of the unit cycle of locomotion. Although we can obviously acquire a better estimate for the speed of displacement through forward acceleration than through vertical acceleration, we used vertical acceleration at initiation and termination of walking because there are significant fluctuations in forward acceleration at the time. This means that the variance (error) in step length became larger at initiation and termination of walking.

2.5 Detection of walking behavior on stairs

The typical pattern for vertical acceleration and the forward pattern observed in going up or down stairs are almost the same as that for walking behavior on a flat floor. Critical differences appear in the pattern for the angular velocity vector when walking up stairs, and in the acceleration gap between the negative and the positive peak for vertical acceleration.

2.5.1 Going up stairs

Human locomotion in going up stairs creates distinguishable differences in angular velocity along with the roll-axis. Figure 10 has a typical pattern for vertical acceleration and angular velocity along with the roll-axis while a subject is going up stairs. We notice that the frequency of angular velocity is almost half that of vertical acceleration.

Figures 11 and 12 show typical patterns for vertical acceleration and angular velocity along with the roll-axis while walking on a flat floor and going down

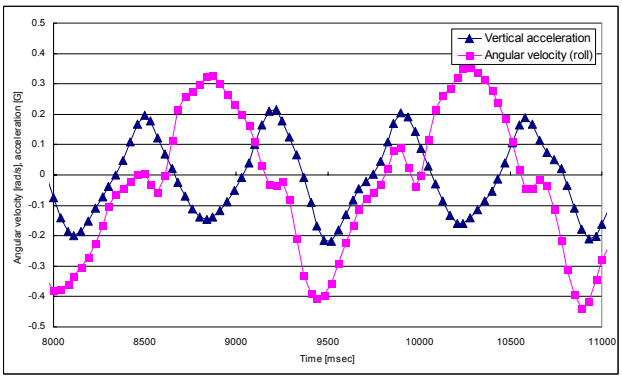

Figure 10: Typical pattern of vertical acceleration and angular velocity (roll-axis) while going up stairs.

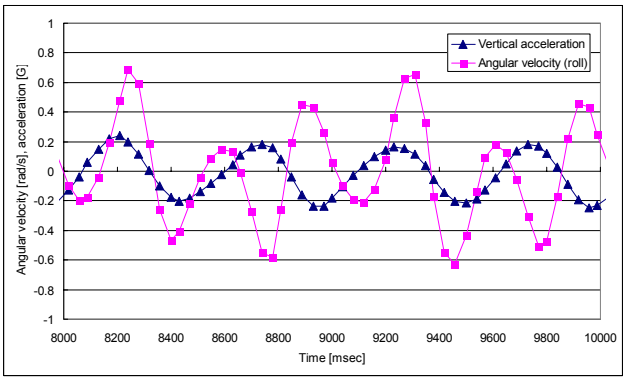

Figure 11: Typical pattern of vertical acceleration and angular velocity (roll-axis) while walking on flat floor.

stairs. It is obvious that the frequency of angular velocity is much larger than (almost 1.5 times) that observed in going up stairs in Figure 10.

2.5.2 Going down stairs

Figure 13 has a typical pattern for vertical and forward acceleration while going down stairs. It is obvious that the difference between the positive and negative peak for the vertical acceleration is much larger than that in walking on a flat floor (Figure 1) and going up stairs (Figure 14).

Therefore, we can distinguish going down stairs from the other walking behaviors.

2.6 Taking an elevator

The motion in an operating elevator is very smooth and well-controlled and thus easy to track. Figure 15 shows the vector length of the acceleration vector filtered with an aggressive low-pass filter (FIR1-type, 50-steps, cut-off frequency: 1/100), while taking a descending elevator, and Figure 16 shows the vertical and forward acceleration. It is noticeable from Fig-

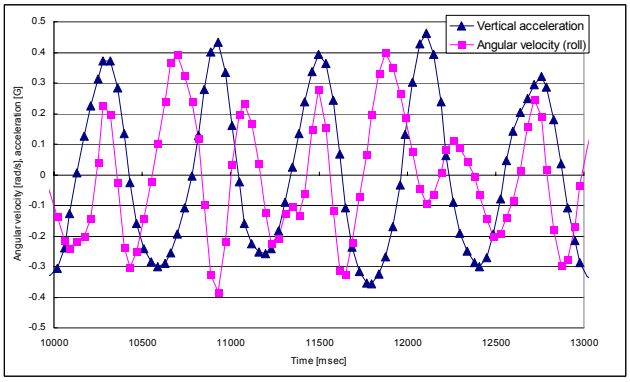

Figure 12: Typical pattern of vertical acceleration and angular velocity (roll-axis) while going down stairs.

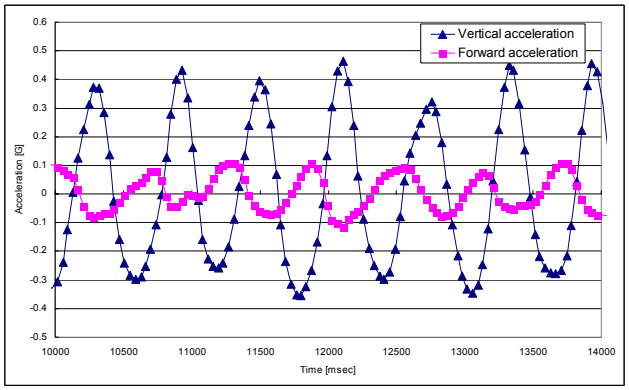

Figure 13: Typical pattern of vertical and forward acceleration while going down stairs.

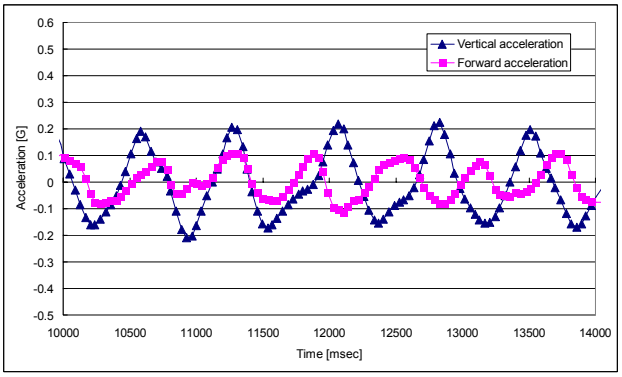

Figure 14: Typical pattern of vertical and forward acceleration while going up stairs.

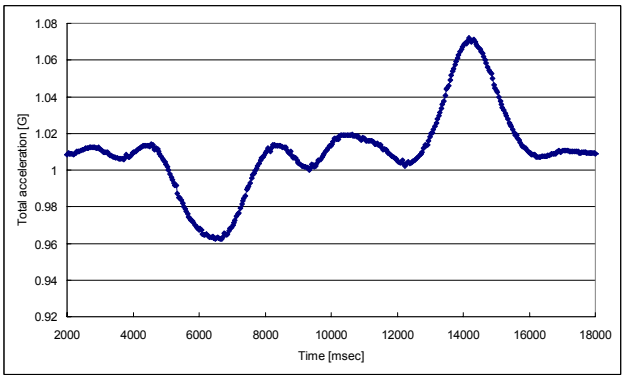

Figure 15: Example of vector length of aggressively low-pass filtered vertical acceleration vector while in descending elevator.

ure 15 that there is a long-range mountain and valley (width: 2000–3000 msec, height 0.04 G) at the start and end of the descent of the elevator although the vertical and forward acceleration are slightly observed.

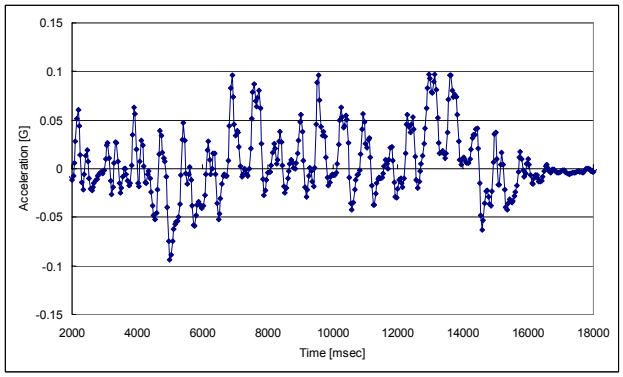

Figure 16: Unfiltered vertical acceleration while in descending elevator in Figure 15.

Figure 17 has an example of the vector length of the aggressively low-pass filtered acceleration vector while walking on a flat floor. We can notice that there is no long-lasting increase or decrease of vector length in the total acceleration vector such as observed in Figure 15 while walking on a flat floor. Therefore, it is not likely that motion will be falsely detected in taking an elevator.

3 Sensor fusion by a Kalman filter framework

In this section, we describe the Kalman filter framework that integrates multiple sources of information that are used to estimate the user's position and orientation. We also describe a method of estimating the absolute position and attitude based on image registration.

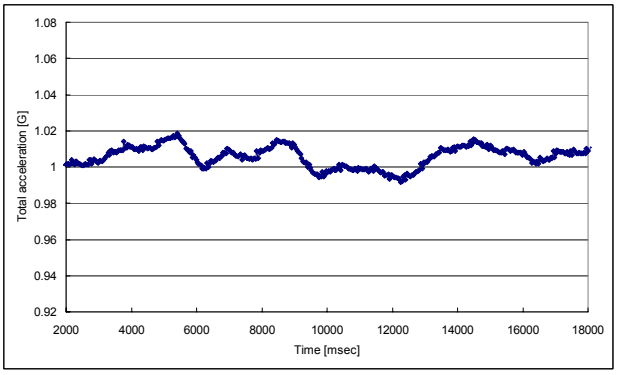

Figure 17: Example of vector length of aggressively low-pass filtered vertical acceleration vector while walking on flat floor.

There are three types of information available to the Kalman filter framework shown below, which are critically required for personal positioning. They are:

1. Absolute attitude (torso),
   The method for estimating gravitational direction is described in Section 2.1, and that for estimating yaw angle is described in the literature [15].

2. Relative displacement by walking,
   The method for estimating the step length is described in Section 2.4.

3. Absolute position and attitude (head).
   The method for estimating the absolute position and attitude of user's head will be described in Section 3.2. We use image registration to estimate this if the current position is covered by the image database, and use a drift-affected inertial head tracker to update it.

We will discuss how this information are fused into a single statistically consistent estimate for user's position and orientation.

3.1 Kalman filter framework

The method integrates data obtained from the wearable camera and the multiple sensors within the Kalman filter into a single output result with a particular uncertainty. The state vector x_k at discrete time k is defined as:

$$x_k = [x_k, y_k, z_k, \alpha_k, \beta_k, \gamma_k, \psi_k, \theta_k, \phi_k]^T, \quad (4)$$

where (x_k, y_k, z_k) is the three-dimensional position of the user, $(\alpha_k, \beta_k, \gamma_k)$ is the absolute attitude of the user's head, and $(\psi_k, \theta_k, \phi_k)$ is the absolute attitude of the user's torso. In this paper, attitude vector is notated by the Euler angle (yaw, pitch and roll). In the Kalman filter framework of a linear system with a control input vector, the state vector is updated by the equation:

$$x_{k+1} = f(x_k) + D_k(x_k)u_k + G_k w_k, \quad (5)$$

where f is a state transition function, w_k is the systematic noise vector and u_k is the control input vector. We apply the dead-reckoning based on human walking to the framework by regarding the control input vector as a walking distance u_k estimated with the method described in Section 2.4, $f(x_k) = x_k$, and $D_k(x_k) = [\cos\psi_k, \sin\psi_k, 0, .., 0]^T$. Because the systematic noise vector w_k is generated by the dead-reckoning estimation, we can assume that $G_k = I$.

The filter equation predicts the optimal estimation of the state vector $\hat{x}_k$ by:

$$\hat{x}_{k+1|k} = f(\hat{x}_{k|k}) + D_k(\hat{x}_{k|k})u_k, \quad (6)$$

where $\hat{x}_{k+1|k}$ is the state vector predicted from the state vector $\hat{x}_{k|k}$ at the previous discrete time.

After the measurement process, $\hat{x}_k$ is updated by the following equation:

$$\hat{x}_{k|k} = \hat{x}_{k|k-1} + K_k[\tilde{y}_k - h(\hat{x}_{k|k-1})], \quad (7)$$

where K_k is Kalman gain, $\tilde{y}_k$ is measurement vector, and h is the prediction function of measurement vector from the state vector. We set the measurement vector $\tilde{y}_k$ acquired from the wearable camera and the multiple sensors as:

$$\tilde{y}_k = [\hat{x}_k, \hat{y}_k, \hat{\alpha}_k, \hat{\beta}_k, \hat{\gamma}_k, \hat{\psi}_k, \hat{\theta}_k, \hat{\phi}_k]^T. \quad (8)$$

Therefore, $h(\hat{x}_k) = \hat{x}_k$. In the Kalman filter framework, the measurement vector and the state vector satisfy:

$$\tilde{y}_k = h(x_k) + v_k, \quad (9)$$

where v_k is measurement noise vector.

Kalman gain K_k is updated by the following equation:

$$K_k = \hat{\Sigma}_{k|k-1}H^T(H\hat{\Sigma}_{k|k-1}H^T + \Sigma_{vk})^{-1}, \quad (10)$$

where $\hat{\Sigma}_k$ is the covariance matrix of the optimal estimation of the state vector $\hat{x}_k$, and Σ_{vk} is the covariance matrix of the measurement noise vector. By the definition of the prediction function $h(x)$, $H = I$.

The covariance equation in the Kalman filter framework updates the covariance matrix $\hat{\Sigma}_k$ by the following equations:

$$\hat{\Sigma}_{k|k} = \hat{\Sigma}_{k|k-1} - K_k H\hat{\Sigma}_{k|k-1}, \quad (11)$$

$$\hat{\Sigma}_{k+1|k} = F\hat{\Sigma}_{k|k}F^T + G_k\Sigma_{wk}G_k^T, \quad (12)$$

where Σ_{wk} is the covariance matrix of systematic noise vector w_k that is configured to be the estimated noise covariance by the regression analysis described in Section 2.4, and by the definition of the state transition function $f(x)$, $F = I$.

When the result of image matching from the wearable camera is available, the user's position $(\hat{x}_k, \hat{y}_k)$ and the absolute attitude of the user's head $(\hat{\alpha}_k, \hat{\beta}_k, \hat{\gamma}_k)$ are given as a part of the measurement vector. The inertial head tracker incrementally gives

the absolute attitude of the user's head $(\hat{\alpha}_k, \hat{\beta}_k, \hat{\gamma}_k)$, and the methods described in Section 2.1 and the literature [15] give the absolute attitude of the user's torso $(\hat{\psi}_k, \hat{\theta}_k, \hat{\phi}_k)$ as measurements.

The measurement noise vector v_k, in the Kalman filter framework, is the discrepancy vector between the measurement vector predicted by the function $h(x)$ and that obtained from real observations by the multiple sensors. The proposed method uses the state vector updated by the dead-reckoning from the previous discrete time as a prediction of the next measurement vector. Thus, the components of the covariance matrix of the absolute attitude incrementally grow because of the drifting effect of the inertial head tracker attached to the user's head. On the other hand, the components of the covariance matrix of the absolute attitude output $(\hat{\psi}_k, \hat{\theta}_k, \hat{\phi}_k)$ should be below a constant and sufficiently small since its estimation uses the gravitational direction and the magnetic vector as the absolute reference.

When the state vector is updated, the accumulation of systematic noise caused by the dead-reckoning based on equation (6) makes the components for the position of the covariance matrix of the optimal estimation of the state vector incrementally grow. Because of the drifting effect of the inertial sensor attached to the head, the components of the absolute attitude of the user's head of the covariance matrix of the measurement noise increase. On the other hand, the components of the absolute attitude of the user's torso should not grow since the components of the measurement noise vector remain constant. When the position and the attitude of the user's head are acquired from image registration, the accumulated components of the position and the absolute attitude of the user's head are thought to shrink below a certain level of accuracy provided by image registration.

Figure 18 shows the system diagram of the Kalman filter described in this section.

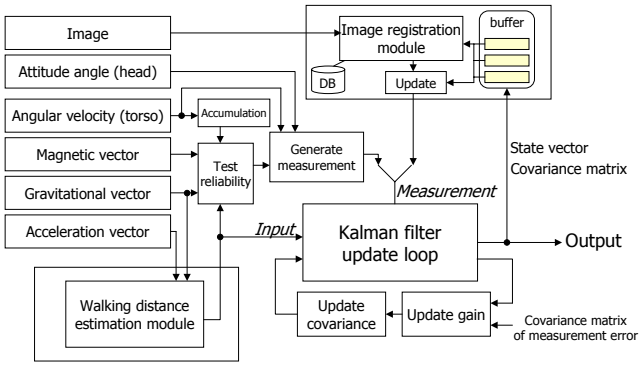

Figure 18: System diagram of the Kalman filter.

3.2 Estimation of position and attitude of head based on image registration

We use a set of images captured at known positions and orientation (attitude) of the camera as an image database. The current position and the attitude of the wearable camera that is attached to the user's head are acquired by image registration between live images from the camera and images in the database. As for the method of image registration, we use the method of estimating global affine parameters between frames described in the literature [14]. After the affine parameters are acquired, we compute the normalized cross correlation of image brightness between the aligned frames with the parameters to determine whether the correlation value exceeds the pre-defined threshold. If it passes the test, image registration is deemed to be successful. When image registration successively matches an input frame and one of the frames in the database, the position and orientation (attitude) of the registered frame are given as measurements to the update loop of the Kalman filter described in Section 3.1.

Since the computational costs involved in image registration are expensive and the image database covers the target area at a sparse density in practice, it is essential to accurately determine the necessity of image registration when an input frame is given at discrete time k. Our method determines this necessity by the optimal estimation of the position and the absolute attitude of the user's head and their components of the covariance matrix $\hat{\Sigma}_k$, which correspond to the uncertainty of the estimation. That is, the method initiates the image registration if any frame is registered in the database whose position and posture are covered by the uncertainty range defined by the optimal estimation and its covariance.

4 Experiment

4.1 Implementation

We implemented a prototype of personal positioning and AR system. Detailed implementation issues of the proposed method are covered by the literature [16]. The following experiments were conducted with the system.

4.2 Walking behavior detection

We tested the recognition of various types of human walking locomotion: (1) walking on a flat floor, (2) going up stairs, (3) going down stairs, and (4) taking an elevator, as described in Section 2.

Table 1 lists the result of accuracy of the recognition by the method. Each number in the table represents a ratio of recognition of a left-shown behavior as a top-shown behavior.

Table 1: Recognition accuracy for four types of behavior.

	Flat	Up	Down	Elevator
Flat	95%	4%	1%	0%
Up	15%	85%	0%	0%
Down	5%	0%	95%	0%
Elevator	0%	0%	0%	100%

Although it is still difficult to completely distinguish between walking on a flat floor, going up/down stairs and taking an elevator (1),(2),(3) and (4), the system's accuracy can be greatly improved by map information on the existence of stairs and elevators.

We also found that the self-contained sensors (3DM-G) could be attached anywhere around the waist since they measured the acceleration vector and angular velocity vector of the pelvis.

4.3 Positioning and annotation overlay

To calibrate the attached attitude of the self-contained sensors (3DM-G) at the initial stage, the subject walked forward a few steps.

Figure 19 has the subject's trajectories estimated with our method not using image registration when walking along the same path of which total distance is 31.4 meter. There are four points where errors in the estimated position and walking distance was measured and these are marked "X". The measured errors are listed in Table 2. This indicates that it can robustly estimate the subject's position and orientation despite the presence of electronic office appliances such as copiers and CRTs, or building structures which disturb the magnetic field.

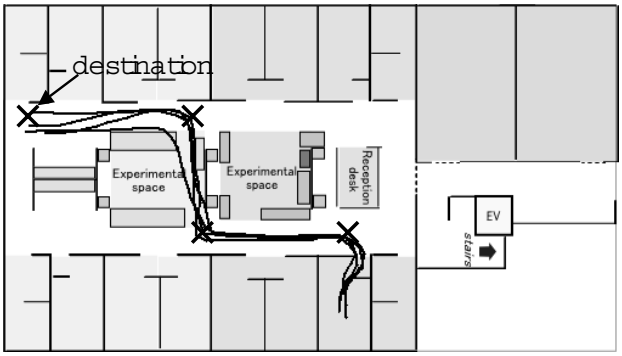

Figure 19: Estimates of trajectories when subject walks along the same path.

Table 2: Errors in estimated position and walking distance [m].

	Point 1	Point 2	Point 3	Point 4
Trial 1	0.2/0.1	0.5/0.6	1.2/1.8	1.7/2.4
Trial 2	0.1/0.0	0.3/0.7	1.0/1.7	1.3/2.0
Trial 3	0.1/0.1	0.4/0.5	2.0/1.6	2.1/2.0
Trial 4	0.1/0.1	0.4/0.6	1.2/1.9	1.4/2.3

Figure 20 has the subject's trajectory estimated with our method in an indoor environment. Here, the estimated position has been adjusted through image registration at the three locations marked with the open circles, and adjusted by detecting the subject's behavior in taking an elevator at the marked location

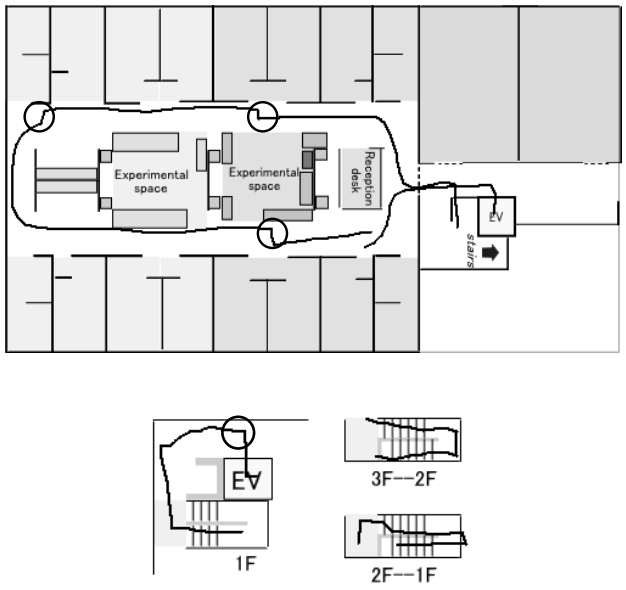

Figure 20: Estimates of trajectory.

in Figure 20 below. In this experiment, the subject first walked around the 3rd floor, and then went down the stairs from the 3rd floor to the 1st floor, and then took an elevator from the 1st floor to the 3rd floor and finally returned to the starting point.

Figure 21 has examples of overlaid annotative information on live video frames based on the estimates of the position and viewing direction of the user.

5 Conclusion

In this paper, we proposed a method of detecting and measuring different types of human walking locomotion and a method of integrating multiple sources of information into a single estimate for position and orientation within a Kalman filter framework.

In future work, we need to adapt individual differences to estimate the walking speed from acceleration. Here, we used a fixed coefficient and intercept statistically obtained from several walking tests. However, we need to eliminate these tests by introducing on-line adaptation.

Although we employed image registration to obtain absolute positioning, a major Japanese railway company has started to deploy Radio Frequency (RF) ID readers at passenger entrances and exits, and thus we assume that the absolute position (and probably direction) of a user will be able to be acquired through these RFID tag readers in the near future.

Acknowledgements

This work is supported in part by Special Coordination Funds for Promoting Science and Technology of MEXT of the Japanese Government and JSPS Postdoctoral Fellowships for Research Abroad (H15).

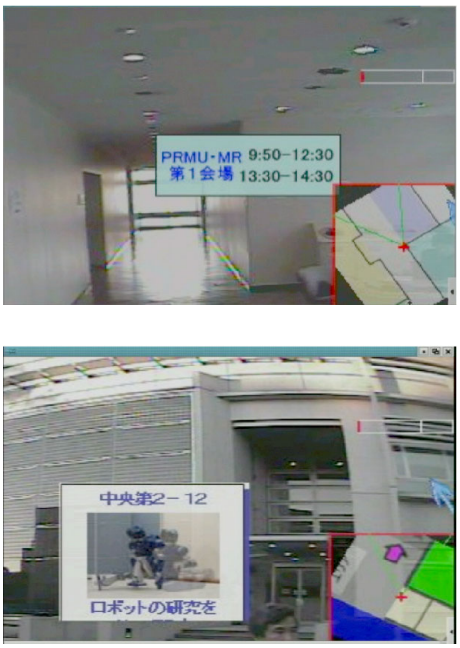

Figure 21: Examples of annotation overlays. (First annotation (above) shows schedule for some oral sessions held in the room, and second (below) shows that robotics research has been conducted in the building (in Japanese).

References

[1] *Weavy: Wearable Visual Interfaces*, `http://www.is.aist.go.jp/weavy/`

[2] Steve Mann, "Wearable Computing: A First Step Toward Personal Imaging," *Computer*, Vol. 30, No. 2, pp. 25–32, 1997.

[3] Steven Feiner, Blair MacIntyre, Tobias Höllerer and Anthony Webster, "A Touring Machine: Prototyping 3D Mobile Augmented Reality Systems for Exploring the Urban Environment," in *Proc. of Int'l Symp. on Wearable Computers (ISWC97)*, pp. 74–81, 1997.

[4] Joseph Newman, David Ingram and Andy Hopper, "Augmented Reality in a Wide Area Sentient Environment," in *Proc. Int'l Symp. on Augmented Reality (ISAR2001)*, pp. 77–86, 2001.

[5] Hisashi Aoki, Bernt Schiele and Alex Pentland, "Realtime Personal Positioning System for Wearable Computers," in *Proc. Int'l Symp. on Wearable Computers (ISWC99)*, pp. 37–43, 1999.

[6] Andrew Golding and Neal Lesh, "Indoor Navigation Using a Diverse Set of Cheap, Wearable Sensors," in *Proc. Int'l Symp. on Wearable Computers (ISWC99)*, pp. 29–36, 1999.

[7] Crossbow Technology, `http://www.xbow.com/`

[8] American GNS Corporation, `http://www.americangnc.com/`

[9] Robert Levi and Thomas Judd, "Dead Reckoning Navigational System Using Accelerometer to Measure Foot Impacts," U.S. Patent Number 5,583,776, 1996.

[10] Thomas Judd, "A Personal Dead Reckoning Module," in *Proc. the Institute of Navigation, GPS'97*, pp. 169–170, 1997.

[11] Point Research Corporation, `http://www.pointresearch.com/`

[12] Seon-Woo Lee and Kenji Mase, "Incremental Motion-Based Location Recognition," in *Proc. Int'l Symp. on Wearable Computers (ISWC2001)*, pp. 123–130, 2001.

[13] Murray MP, "Gait as a total pattern of movement," in *American Journal of Physiological Medicine*, pp. 290–333, 1967.

[14] Masakatsu Kourogi, Takeshi Kurata, Jun'ichi Hoshino and Yoichi Muraoka, "Real-time image mosaicing from a video sequence," in *Proc. Int'l Conference on Image Processing (ICIP99)*, Vol. 4, pp. 133–137, 1999.

[15] Masakatsu Kourogi and Takeshi Kurata, "A method of personal positioning based on sensor data fusion of wearable camera and self-contained sensors," in *Proc. IEEE Conference on Multisensor Fusion and Integration for Intelligent Systems (MFI2003)*, pp. 287–292, 2003.

[16] Masakatsu Kourogi and Takeshi Kurata, "A Wearable Augmented Reality System with Personal Positioning based on Walking Locomotion Analaysis," in *Proc. Int'l Symp. on Mixed and Augmented Reality (ISMAR2003)*, pp. 342–343, 2003.

[17] MicroStrain Inc., `http://www.microstrain.com/`

[18] Robert Brown and Patrick Hwang, "Introduction to random signals and applied Kalman filtering," Wiley, 1997.

[19] Andrew Davidson, "Mobile Robot Navigation Using Active Vision," in *Ph. D thesis in University of Oxford*, 1999.